Contract No. and Disclaimer:

This manuscript has been authored by Savannah River Nuclear Solutions, LLC under Contract No. DE-AC09-08SR22470 with the U.S. Department of Energy. The United States Government retains and the publisher, by accepting this article for publication, acknowledges that the United States Government retains a non-exclusive, paid-up, irrevocable, worldwide license to publish or reproduce the published form of this work, or allow others to do so, for United States Government purposes.

Bimetallic Lithium Borohydrides toward Reversible Hydrogen Storage

Ming Au[1,*], Mohammed J. Meziani,[2] Ya-Ping Sun[2], Frederick.E.Pinkerton[3]

[1]Savannah River National Laboratory, Aiken, SC, USA, [2]Clemson University, Clemson, SC, USA and [3]General Motors R&D Center, Warren, MI, USA

Abstract

Borohydrides such as $LiBH_4$ have been studied as candidates for hydrogen storage because of their high hydrogen contents (18.4 wt% for $LiBH_4$). Limited success has been made in reducing the dehydrogenation temperature by adding reactants such as metals, metal oxides and metal halides [1-5]. However, full rehydrogenation has not been realized because of multi-step decomposition processes and the stable intermediate species produced. It is suggested that adding second cation in $LiBH_4$ may reduce the binding energy of B-H. The second cation may also provide the pathway for full rehydrogenation. In this work, several bimetallic borohydrides were synthesized using wet chemistry, high pressure reactive ball milling and sintering processes. The investigation found that the thermodynamic stability was reduced, but the full rehydrogenation is still a challenge. Although our experiments show the partial reversibility of the bimetallic borohydrides, it was not sustainable during dehydriding-rehydriding cycles because of the accumulation of hydrogen inert species.

Key words: Borohydride, Hydrogen, Storage, Reversibility, Stability, Rehydrogenation, Dehydrogenation

1. INTRODUCTION

Lithium borohydride, $LiBH_4$, has both high gravimetric (18.4 wt%) and volumetric (121 kg/m^3) hydrogen densities making it a potential candidate as a hydrogen storage material. The release of hydrogen from $LiBH_4$ requires temperatures in excess of 300^oC and rehydrogenation requires both high temperatures (>650^oC) and pressure (>190 bar) [1]. A number of recent papers have reported decreases in dehydriding temperatures (or destabilization) by mixing $LiBH_4$ with additives such as metal oxides [2,3], metal halides [4], metal hydrides [5], metal complex hydrides [6,7], carbon [8] and metals [1,9,10]. In spite of many other reports on decrease of dehydrogenation temperature, it is a crucial question if the modified $LiBH_4$ can repeatedly absorb hydrogen after dehydrogenation.

Several metal borohydrides with lower dehydriding temperature such as $Zr(BH_4)_2$, $Ti(BH_4)_3$, $Mn(BH_4)_2$, $Mg(BH_4)_2$ and $Al(BH_4)_3$ have been synthesized through organic wet chemical reactions [11-16]. Historically, the volatile metal borohydrides such as $Cr(BH_4)_3$, $Zn(BH_4)_2$, and $Sn(BH_4)_2$ [17-19] have been used for generation of diborane, B_2H_6, which is a precursor for boron chemical vapor deposition. Recently, these metal

* Corresponding author: ming_au@srnl.doe.gov, 803-507-8547

borohydrides have been investigated for reversible hydrogen storage. These borohydrides either desorbed hydrogen at high temperature (above 250^{o}C) or evolved significant diborane (B_2H_6) gas. Diborane emission was observed from unstable $Mg(BH_4)_2$ and $Mn(BH_4)_2$ as well [20,21]. None of these borohydrides appears to be reversible under practical temperatures and pressures.

It is realized that the thermodynamic stability of metallic borohydrides represented by dehydriding temperature is determined by their composition and structure at the molecular level. Less electronegative metal borohydrides such as KBH_4 (χ=0.82), $NaBH_4$ (χ=0.93) and $LiBH_4$ (χ=0.98), where χ is the Pauling electronegativity, are very stable. Meanwhile, more electronegative metal borohydrides such as $Al(BH_4)_3\uparrow$ (χ=1.61), $Zn(BH_4)_2$ (χ=1.65) and $Ti(BH_4)_3$ (χ=1.54) are very unstable. It is known that the charge transfer (electron density) determines the ionic character of M-BH_4 bonds [22]. By partially substituting a less electronegative metal (M^a: Li,Na,K) with more electronegative metal (M^b: Zn, Ti, Mn, Zr, Mg) may tune the bond of M^aM^b-BH_4 to less ionic that allows finding a middle ground - the less stable bimetallic borohydrides. In this exploratory work, the research was focused on synthesis of the bi-metallic borohydrides and performance evaluation. The experimental results and related discussion are presented in this paper.

2. EXPERIMENTAL DETAILS

2.1 Precursors of materials

The LiH (99% purity), $NaBH_4$, $LiBH_4$, FeB, TiB_2, CrB_2, ZrB_2, MgB_2, NiB and $B_{10}H_{14}$ (99.9-99.99% purity) were purchased from Sigma-Aldrich and used directly without pre-treatment. $ZnCl_2$, $MgCl_2$ and $TiCl_4$ were purchased from Alfa Aesar. The solvents diethyl ether, toluene, and hexane were distilled over sodium metal before use. Other solvents were either spectophotometry/HPLC grade or purified via simple distillation. Deuterated NMR solvents were obtained from Cambridge Isotope Laboratories.

2.2. Ball milling-sintering process

Three grams of the appropriate LiH, $B_{10}H_{14}$ and metal boride powder mixture were placed in a 45 mL hardened steel grinding bowl with four 6 mm diameter steel balls. The sealed grinding bowls were taken out of the argon glove box and put on Frisch-7 planetary ball mill for 1 hour milling at 200 rpm. After milling, the powders were transferred to a Parr vessel for 48 hour sintering at 200 - 400^{o}C and 100 bars H_2. After completion of sintering, the materials were examined by XRD and TGA-RGA for their phase compositions and hydrogen storage behavior.

2.3 High pressure ball milling process

Duplicates of the above mixtures were loaded in EvicoMagetic grinding vial, pressurized to 100 bar H_2 and milled at 400 rpm in Frisch-6 planetary ball mill (Fig.1a). The pressure

and temperature sensors measured and transmitted the information to a computer for real time monitoring. The hydrogenation can be evidenced by the pressure decrease (Fig.1b).

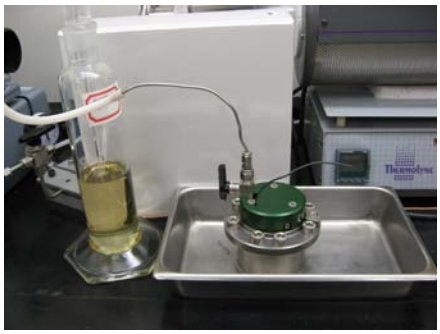

Fig. 1 (a) Hydrogen releasing from the high pressure vial

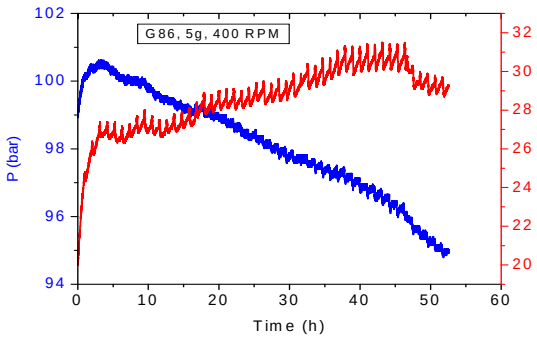

Fig.2 (b) The P-T-t correlation during ball milling of G86 material

2.4 Wet chemistry process

$Li_2Mg(BH_4)_4$, $Li_{1.3}Mg(BH_4)_{3.3}$ and $TiMg_{3.4}(BH_4)_{9.8}$ were prepared by reacting relatively stable $Mg(BH_4)_2{\cdot}2Et_2O$ with additional metal chloride compounds under otherwise similar experimental conditions. All experiments were performed in an argon filled glove box.

2.4.1 Prepare $Mg(BH_4)_2$

$NaBH_4$ (9.6 g, 252 mmol) and $MgCl_2$ (6 g, 63 mmol) were mixed and stirred into pre-degassed diethyl ether (100 mL) at room temperature in an argon filled glove box. The mixture was refluxed in diethyl ether (~35 °C) for 3 days. After the reaction, the solution was cooled to room temperature and the mixture was filtered and rinsed with diethyl ether. The filtrate was collected and evaporated under vacuum to yield $Mg(BH_4)_2{\cdot}2Et_2O$ as transparent oily liquid (8.6 g, 68% yield). The chemical purity of the $Mg(BH_4)_2{\cdot}2Et_2O$ compound was confirmed by ^{11}B NMR, from which the results (δ -43.1 ppm, $J_{B\text{-}H}$ = 81.8 Hz, with $BF_3{\cdot}Et_2O$ as an external standard) agreed well with those already in the literature (δ -42.8 ppm, $J_{B\text{-}H}$ = 83.0 Hz) [23].

A portion of the $Mg(BH_4)_2{\cdot}2Et_2O$ sample (2 g, 9.9 mmol) was dissolved in pre-degassed toluene (15 mL), and the solution was refluxed (~110 °C) overnight in the argon filled glove box. The white precipitate was collected and then dried at 110 °C to obtain $Mg(BH_4)_2$ as a white powder (0.5 g, 94% yield).

2.4.2 Prepare $Li_2Mg(BH_4)_4$ and $Li_{1.3}Mg(BH_4)_{3.3}$

$LiBH_4$ (0.405 g, 18.43 mmol) was dissolved in pre-degassed diethyl ether (20 mL) and mixed with $Mg(BH_4)_2{\cdot}2Et_2O$ (1.86 g, 9.22 mmol). The mixture was stirred at room temperature overnight in the glove box. After the removal of diethyl ether under vacuum,

the product was dissolved in pre-degassed toluene (10 mL), and the solution was refluxed (~110 °C) for 3 h. The white precipitate was collected and then dried at 120 °C to obtain $Li_2Mg(BH_4)_4$ as a white powder (860 mg), as confirmed by the elemental analysis.

The same procedure was used to prepare $Li_{1.3}Mg(BH_4)_{3.3}$ by simply changing the molar ratio of $LiBH_4$ to $Mg(BH_4)_2{\cdot}2Et_2O$ to 1:1. Both bimetallic borohydrides were found to give rise to a highly exothermic reaction when in contact with water.

2.4.3 Prepare $TiMg_{3.4}(BH_4)_{9.8}$

$Mg(BH_4)_2{\cdot}2Et_2O$ (1.212 g, 6 mmol) was dissolved in pre-degassed diethyl ether (10 mL) and stirred in the glove box. To the solution was added $TiCl_4$ (379 mg, 2 mmol) dropwise, and the mixture was stirred overnight at room temperature. The solution changed from colorless to blue and then dark-blue. After the reaction, the mixture was filtered and the filtrate was collected and evaporated under vacuum. The product was then dissolved in pre-degassed hexane (10 mL), and the solution was refluxed (~70 °C) for 2 h. The precipitate was collected and then dried at 90 °C to obtain $TiMg_{3.4}(BH_4)_{9.8}$ as a black powder (850 mg), as determined by the elemental analysis.

2.5 Materials characterization

An SRS RGA-300 Residual Gas Analyzer (RGA) coupled with a Perkin Elmer Pyris-1 Thermal Gravimetric Analyzer (TGA) was used to measure the weight loss and analyze the composition of the gases evolved during thermal decomposition, simultaneously. Five mg of samples were used in the TGA for each measurement. Research grade Argon with a purity of O_2<0.1ppm, H_2<0.1ppm, H_2O<0.5ppm, N_2<0.1ppm, total hydrocarbon (THC)<0.1ppm and ($CO+CO_2$) < 0.1 ppm was passed at 60 ml/min from the TGA through a 3.2mm OD PEEK™ tubing to the RGA instrument. The targeted evolving gases monitored by RGA were H_2O(18), H_2(2), O_2(32) and B_2H_6(26). The simultaneous TGA-RGA measurement determined the critical desorption temperature, weight loss and evolved gas composition during thermal decomposition. After TGA-RGA pre-screening, 0.5 g samples were transferred to a 5 mL sample holder connected with the 2 liter desorption chamber of a Sieverts apparatus. The system was evacuated to 5 mbar before temperature programmed desorption (TPD) initiated. An MKS vacuum transducer measured subsequent pressure changes. The temperature was increased from ambient to 500°C at 5°C/min. Rehydriding was conducted isothermally at 500°C and 70 bar utilizing 99.9999% hydrogen. The hydrogen absorption and desorption capacities were calculated based on the total sample mass including the additives. The samples were analyzed by X-Ray Diffraction analysis (XRD) on a Scintag XDS-2000 powder diffraction system to determine phase compositions in the three states: as synthesized, dehydrided and rehydrided. Solid-state magic angle spinning (MAS) nuclear magnetic resonance (NMR) spectra were measured on a Bruker Advance 500 NMR spectrometer and at the California Institute of Technology using a Bruker Avance 500 MHz spectrometer with a wide bore 11.7 T magnets and employing a boron-free Bruker 4 mm probe. FT-IR spectra were obtained on a Nicolet Magna-IR 550 FT-IR spectrometer. Samples for measurements were mixed with carefully dried KBr, and the solid mixture was then made

into pellets using a 13-mm die and a hydraulic press. All measurements were carried out under the protection of dry nitrogen gas.

3. RESULTS AND DISCUSSION

3.1 Bi-metallic borohydride synthesized by high temperature sintering process

In attempt to synthesize bimetallic borohydrides $Li_{1.5}Ti_{0.5}(BH_4)_3$, $Li_{1.5}Fe_{0.5}(BH_4)_3$, $Li_{1.5}Cr_{0.5}(BH_4)_{4.5}$ and $LiMg_{0.5}(BH_4)_2$, four powder mixtures $1.5LiH+0.5TiB_2+0.2B_{10}H_{14}$, $1.5LiH+0.5TiB_2+0.2B_{10}H_{14}$, $1.5LiH+0.5CrB_2+0.35B_{10}H_{14}$ and $LiH+0.5MgB_2+0.3B_{10}H_{14}$ were sintered respectively at different temperatures and pressures depending on their volatility. The results of their characterization and hydrogen storage performance are stated below.

3.1.1 Bi-metallic borohydride $Li_{1.5}Ti_{0.5}(BH_4)_3$

Targeting the bi-metallic borohydride $Li_{1.5}Ti_{0.5}(BH_4)_3$, three grams of the mixture $1.5LiH+0.5TiB_2+0.2B_{10}H_{14}$ was sintered at 200°C and 120 bars for 48 hours. XRD indicates that there is no reaction of the precursors. The LiH and TiB_2 remain unchanged with the decomposition of $B_{10}H_{14}$. A small amount of LiOH was formed due to absorption of the moisture introduced in sample handling (Fig.9).

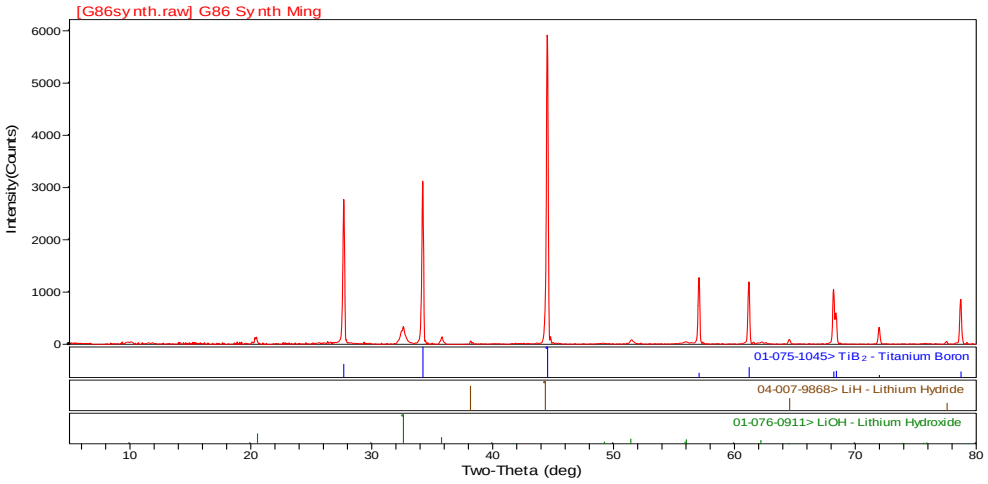

Fig.9 XRD of sintered mixture of $1.5LiH+0.5TiB_2+0.2B_{10}H_{14}$

The sintered sample was investigated by TGA-RGA. The results show that material lost 4 wt% starting from 550°C. There are two dehydriding peaks at 620°C and 680°C that may correspond to interaction of LiH and TiB_2 and the decomposition of LiH (689°C) respectively (Fig. 10) [5]. It supports XRD conclusion that the precursors did not react each other during sintering.

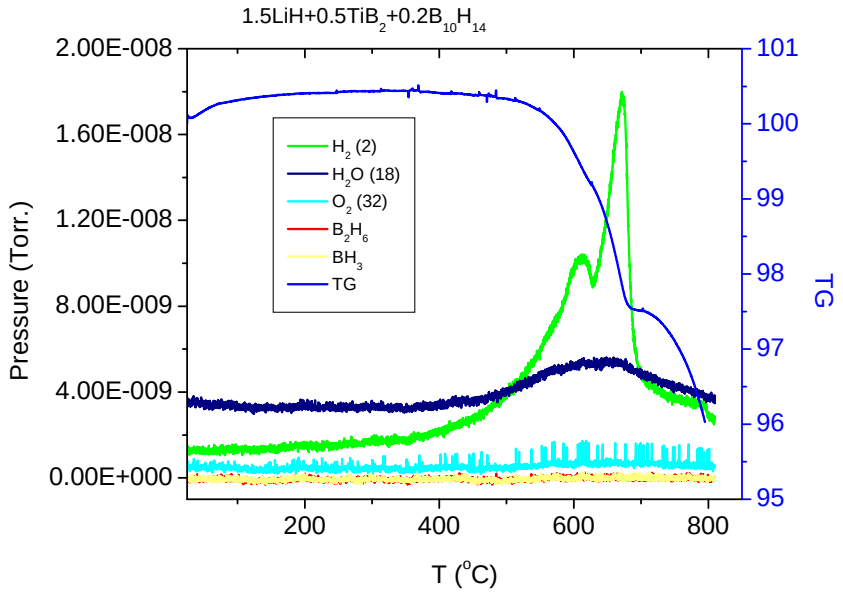

Fig.10 TGA-RGA of 1.5LiH+0.5TiB$_2$+0.2B$_{10}$H$_{14}$ sintered at 300°C

The sample1.5LiH+0.5TiB$_2$+0.2B$_{10}$H$_{14}$ (sintered at 300°C) desorbed 8 wt% H_2 at 600°C and 8 mbar (Fig.11) and reabsorbed same amount of hydrogen at 600°C and 120 bar (Fig.12). Further investigation found that the sample did not release hydrogen below 500°C. Although the sample demonstrates rehydrogenation capability, the operating conditions are too high for practical application.

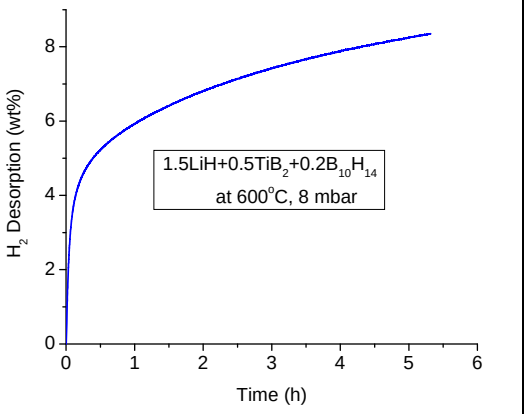

Fig.11 Dehydriding of 1.5LiH+0.5TiB$_2$+0.2B$_{10}$H$_{14}$

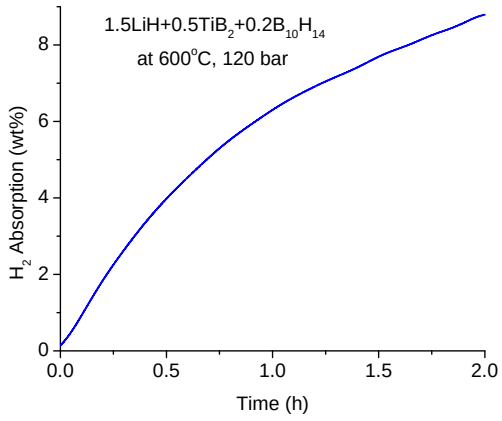

Fig.12 Rehydriding of 1.5LiH+0.5TiB$_2$+0.2B$_{10}$H$_{14}$

3.1.2 Bi-metallic borohydride $Li_{1.5}Fe_{0.5}(BH_4)_3$

Three grams of the mixture 1.5LiH+0.5FeB+0.25B$_{10}$H$_{14}$ was sintered at 400°C and 100 bars for 48 hours. After sintering, the powder mixture was transformed to a gray solid mass.

XRD detected $LiBH_4$, Fe_2B and B in addition to remaining precursors LiH and FeB. It indicates that the B reacted with LiH and formed $LiBH_4$. Some of boron possibly derived from FeB (2FeB → Fe_2B +B) or $B_{10}H_{14}$ ($B_{10}H_{14}$ →10B+7H_2). There are several relatively weak unidentified peaks at 2θ = 9, 9.5, 11.5, 12, 30.5, 39.5 (Fig.13). Our hypotheses are: 1) the reaction LiH+B+H_2 →$LiBH_4$ occurred in relatively moderate conditions because of the fresh B generated from *in-situ* boride decomposition; 2) the reaction did not complete at these conditions, 3) most of the Fe was still bound with B in Fe_2B. However, the existence of $LiFe_x(BH_4)_y$ can not be ruled out until the unknown peaks are identified.

The sintered 1.5LiH+0.5FeB+0.25$B_{10}H_{14}$ was investigated by TGA-RGA. TGA measured 3% weight loss up to 550°C. RGA did not detect other gases except H_2. Therefore, the 3% weight loss should be attributed to H_2 evolution from decomposition of $LiBH_4$ or possible a bimetallic borohydride such as $LiFe_x(BH_4)_y$ (Fig.14).

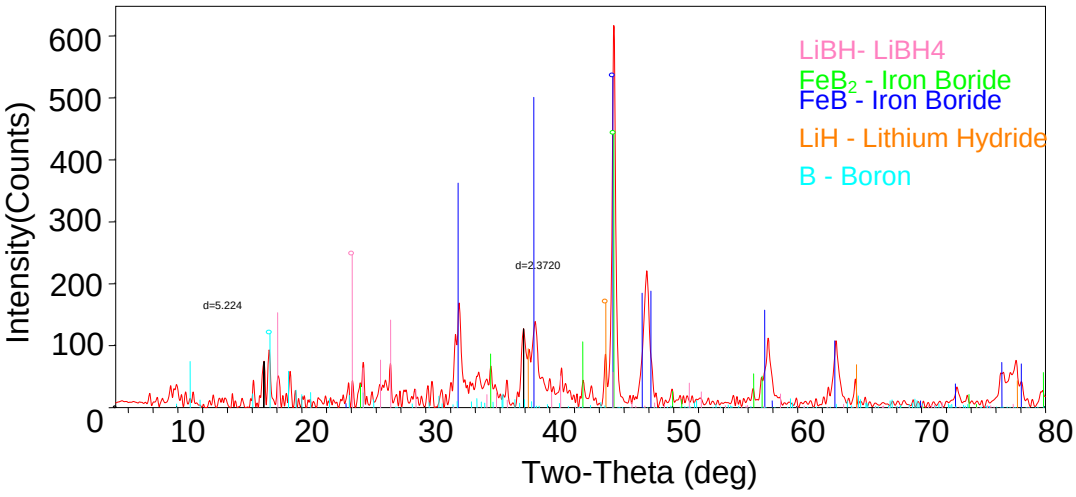

Fig.13 XRD of sintered 1.5LIH+0.5FeB+0.25$B_{10}H_{14}$

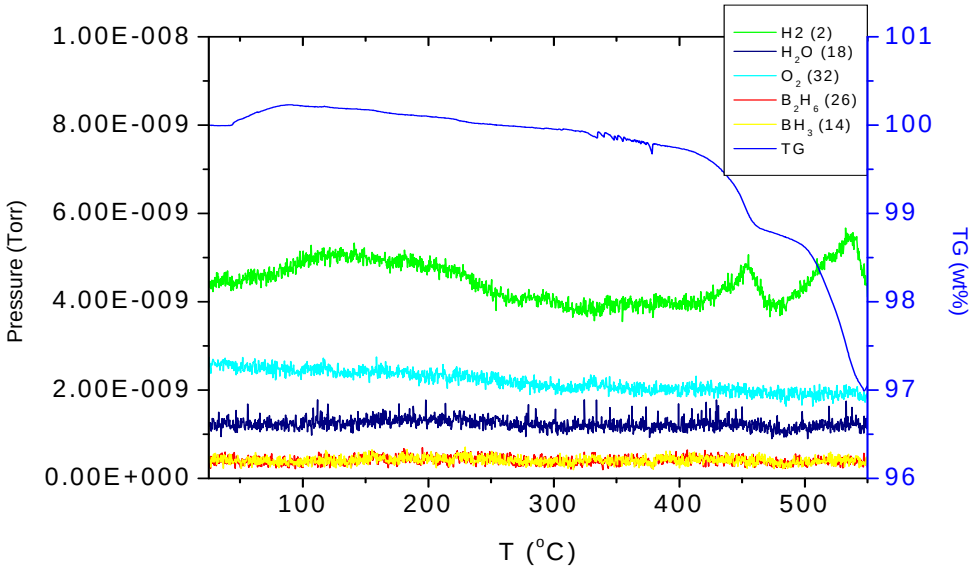

Fig.14 TGA-RGA of sintered $1.5LIH+0.5FeB+0.25B_{10}H_{14}$

Three H_2 peaks at 150°C, 450°C and 540°C were observed in RGA spectra. The first small peak between 100°C-200°C may correspond to phase transformation of $LiBH_4$. At 350°C, several bumps in TG curve indicate melting of sample. It is known that $LiBH_4$ melts at 280°C. The bumps may correspond to melting of speculated $LiFe_x(BH_4)_y$. It is noted that the sample was molten after 350°C. The dehydrogenation took place at liquid state where the borohydride became an ionic liquid consisted of Li^+, $[BH_4]^-$, [B], Fe^{+3} and LiH. The peak at 400°C seems relating to decomposition of $[BH_4]^- \rightarrow B + 2H_2$. The peak at 550°C may relate to decomposition of the unknown compound such as speculated $LiFe_x(BH_4)_y$.

The isothermal dehydrogenation and rehydrogenation show that the sample $1.5LiH+0.5FeB+0.25B_{10}H_{14}$ desorbed 4 wt% H_2 at 450°C and 1 bar in 30 hours and reabsorbed same amount of H_2 at 450°C and 100 bar in 16 hours (Fig.15-16). It implies that the material may be reversible at the conditions. However, the capacity and the reaction kinetics are not attractive.

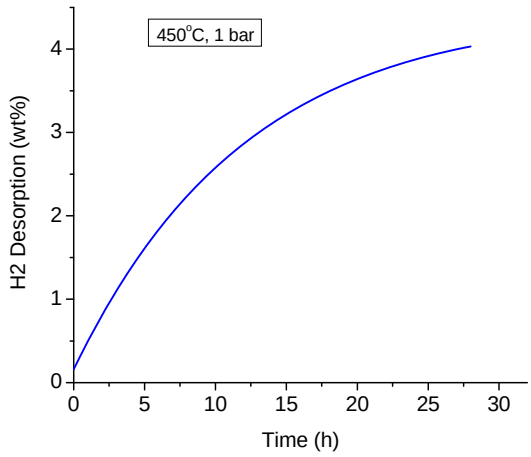

Fig.15 Dehydrogenation of 1.5LIH+0.5FeB+0.25$B_{10}H_{14}$

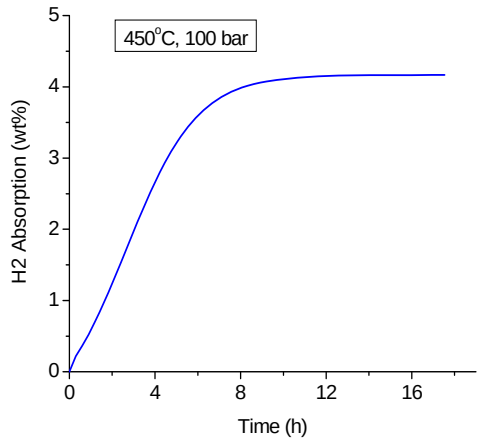

Fig.16 Rehydrogenation of1.5LIH+0.5FeB+0.25$B_{10}H_{14}$

3.1.3 Bi-metallic borohydride $Li_{1.5}Cr_{0.5}(BH_4)_{4.5}$

Targeting the bi-metallic borohydride $Li_{1.5}Cr_{0.5}(BH_4)_{4.5}$, three grams of the mixture $1.5LiH+0.5CrB_2+0.35B_{10}H_{14}$ were sintered at 400°C and 100 bars for 48 hours. After sintering, the powder mixture was transformed to a gray solid mass.

XRD detected LiOH and CrB_2 with LiH and $B_{10}H_{14}$ disappeared (Fig.17). The peak at $2\theta = 9.055$ can not be identified with existing database. It shows that some unknown species such as $Li_{1.5}Cr_{0.5}(BH_4)_{4.5}$ may form. The polyethylene film may not be sufficient to prevent moisture permeating to XRD sample resulting in formation of LiOH.

TGA measured 4.5 wt% weight lose starting from 350°C. There are two dehydriding peaks at 430°C and 680°C that may correspond to decomposition of the unknown species and the decomposition of LiH (689°C) respectively (Fig.18).

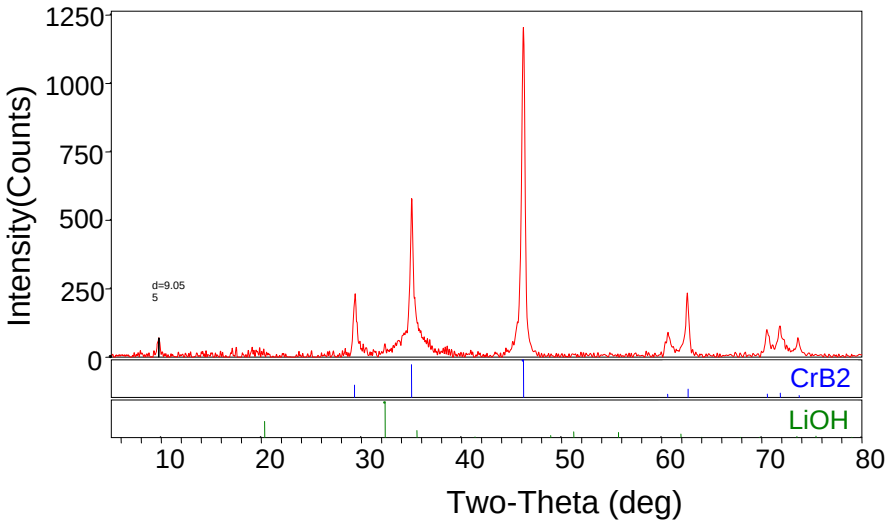

Fig.17 XRD of sintered mixture of $1.5LiH+0.5CrB_2+0.35B_{10}H_{14}$

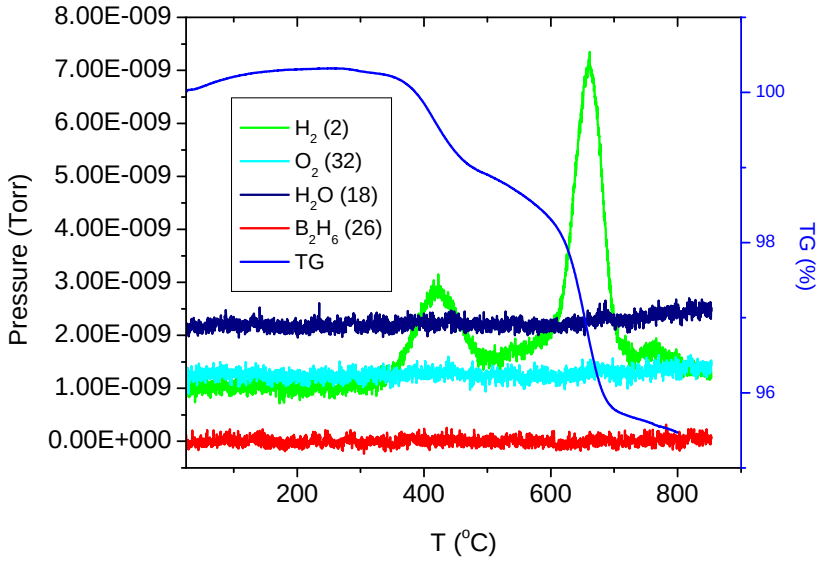

Fig.18 TGA-RGA of sintered mixture of $1.5LiH+0.5CrB_2+0.35B_{10}H_{14}$

0.5 g of sample was loaded in Sieverts apparatus to measure isothermal dehydriding and rehydriding properties. The sample desorbed 2.6 wt% H_2 at 500°C in 2 hours and 1 bar (Fig.19) and reabsorbed 3.0 wt% H_2 at 500°C and 100 bars in 3.5 hours (Fig.20). With high dehydrogenation temperature and low reversible capacity, this material does not show promising.

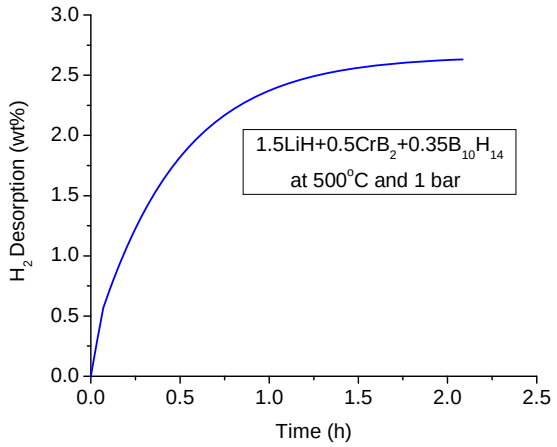

Fig.19 H_2 desorption of $1.5LiH+0.5CrB_2+0.35B_{10}H_{14}$

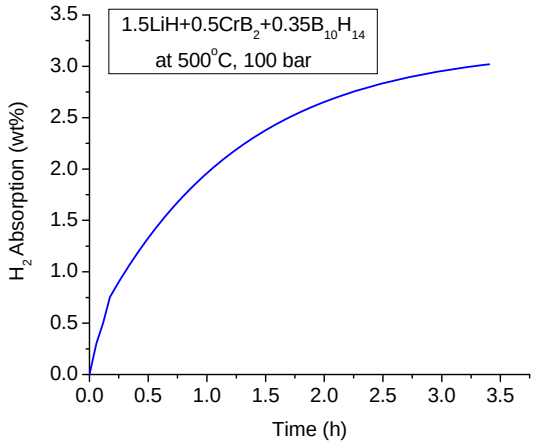

Fig.20 H_2 absorption of $1.5LiH+0.5CrB_2+0.35B_{10}H_{14}$

3.1.4 Bi-metallic borohydride $LiMg_{0.5}(BH_4)_2$

Targeting the bi-metallic borohydride $LiMg_{0.5}(BH_4)_2$, three grams of the mixture $LiH+0.5MgB_2+0.3B_{10}H_{14}$ were sintered at 400°C and 100 bar for 48 hours. XRD identified MgB_2, MgH_2, $Li_2B_4O_7.5H_2O$ and $H_2B_{12}(OH)_{12}$ (Fig.21). The formation of MgH_2 and disappearance of LiH indicates the reaction of $2LiH + MgB_2 + 4H_2 \rightarrow 2LiBH_4 + MgH_2$ took place during sintering [6]. However, Mg did not coordinate with B-H specie to form desired bi-metallic borohydride $LiMg_{0.5}(BH_4)_2$. The poorly prepared XRD sample suffered hydrolysis and therefore some of $LiBH_4$ transformed to $Li_2B_4O_7.5H_2O$. It was noted that there are eight small peaks unidentified from 2θ 10° to 30°. These peaks could not be assigned from the existing index database, but may be the indications of new compounds such as $LiMg_{0.5}(BH_4)_2$. Comparing these results, it is realized that the borides with lower melting point, such as FeB (1650°C) and MgB_2 (800°C), tend to react with LiH at same pressure and temperature.

TGA measured 8 wt% weight loss from 300°C to 500°C and another 8 wt% from 500°C to 700°C (Fig.22). There are three dehydriding peaks in RGA spectra. The peaks at 350°C, 450°C and 630°C may correspond to dehydrogenations of MgH_2, $LiBH_4$ and LiH respectively.

0.4 g of sintered $LiH+0.5MgB_2+0.3B_{10}H_{14}$ was loaded in Sieverts for isothermal dehydriding and rehydriding. It desorbed 2.5 wt% H_2 at 500°C and 8 mbar in 20 hours (Fig.23) and reabsorbed 5.5 wt% H_2 at 500°C and 80 bar in 6 hours (Fig.24). As observed, the material absorbed more hydrogen than what it released at same temperature due to poor desorption kinetics.

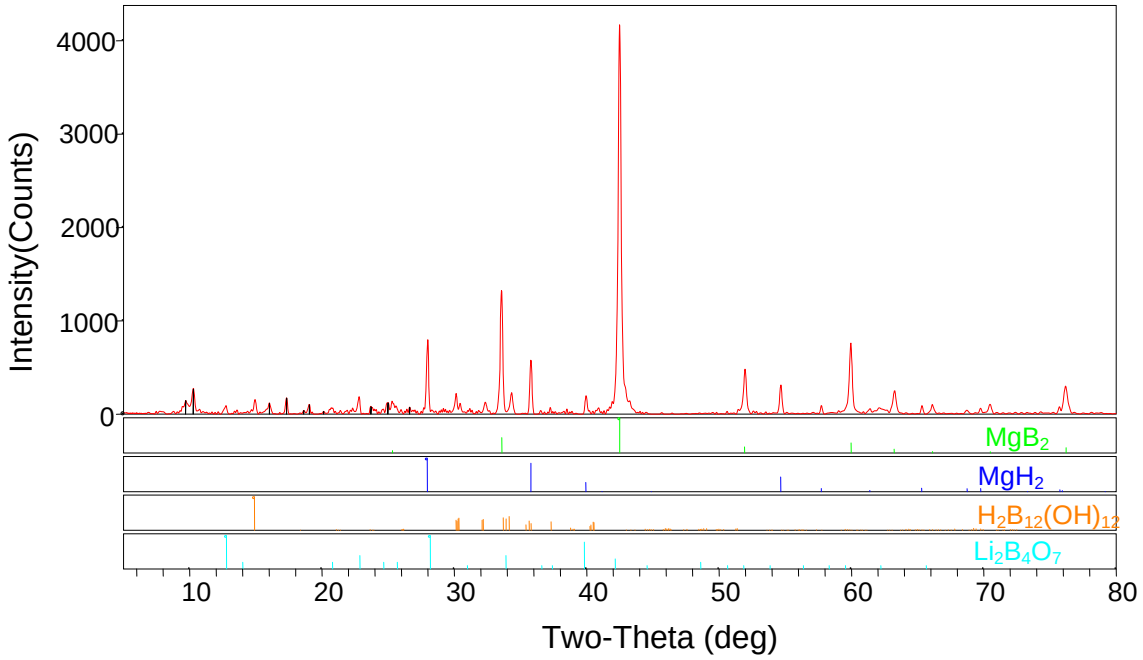

Fig.21 XRD of sintered mixture of $LiH+0.5MgB_2+0.3B_{10}H_{14}$

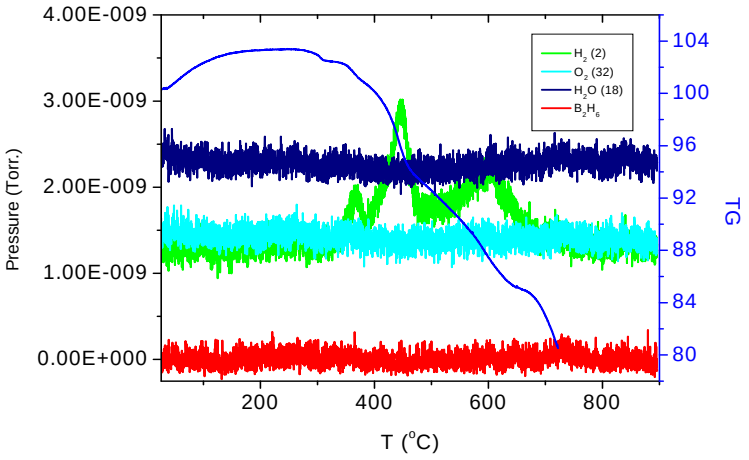

Fig.22 TGA-RGA of sintered $LiH+0.5MgB_2+0.3B_{10}H_{14}$

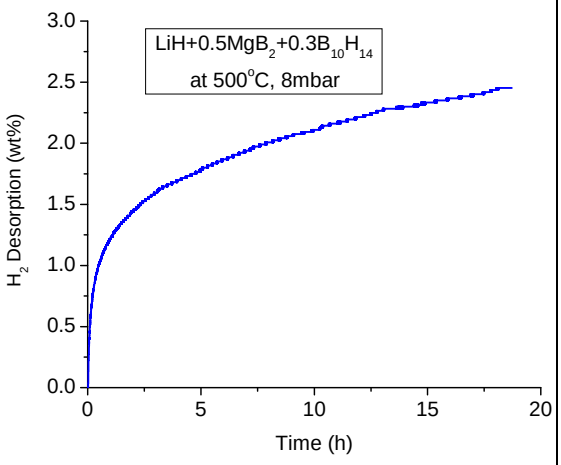

Fig.23 Dehydriding of sintered $LiH+0.5MgB_2+0.3B_{10}H_{14}$

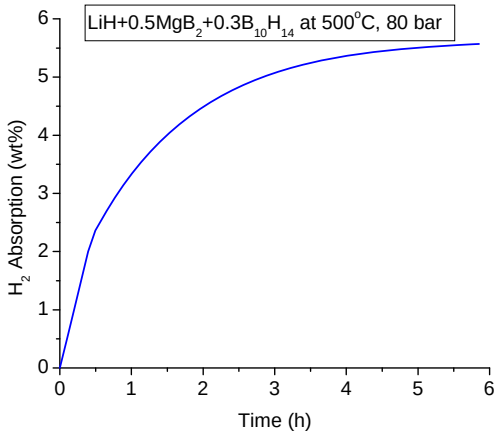

Fig.24 Rehydriding of sintered $LiH+0.5MgB_2+0.3B_{10}H_{14}$

In summary, the high temperature and high pressure sintering promoted interaction of the lithium hydride, decaborane, hydrogen and metal borides with low melting point, such as FeB and MgB_2. The reaction produced $LiBH_4$ and the new compounds that can not be confirmed as the bimetallic borohydrides yet. The dehydriding temperature of the sintered samples is about 400°C that is same as the $LiBH_4$. However, the dehydriding and rehydriding capacities (2.5 ~ 8 wt%) are lower than $LiBH_4$ (12 wt%). It seems that the solid reaction of the precursors at high temperature and pressure is not an efficient approach to synthesize bimetallic borohydrides expected with moderate operating conditions and sufficient hydrogen storage capacity.

3.2 Bi-metallic borohydride synthesized by high pressure ball milling process

To compare the synthesis efficiency with high pressure sintering process, two samples, $1.5LiH+0.5TiB_2+0.2B_{10}H_{14}$ and $LiH+0.5MgB_2+0.3B_{10}H_{14}$, were ball milled at 100 bar H_2 for 100 hours.

The XRDs show no metal borohydrides formed in two samples. The precursors LiH, TiB_2 and MgB_2 were clearly identified (Supporting Fig.1-2). The precursor $B_{10}H_{14}$ seems decomposed and disappeared from XRD spectra.

TGA-RGA measured 1 wt% and 3 wt% loss for ball milled $LiH+0.5MgB_2+0.3B_{10}H_{14}$ and $1.5LiH+0.5TiB_2+0.2B_{10}H_{14}$ respectively. There were no notable hydrogen evolutions detected by RGA (Supporting Fig.3-4). However, with same compositions the sintered samples $LiH+0.5MgB_2+0.3B_{10}H_{14}$ and $1.5LiH+0.5TiB_2+0.2B_{10}H_{14}$ show 20 wt% and 4 wt% of weight loss and typical dehydriding peaks (Fig. 22 and Fig.10).

It is concluded that the high pressure ball milling does not seem as an effective technique to synthesize bimetallic borohydrides because of the conditions is not inadequate for substantial chemical reactions of the precursors.

3.3 Characterization of bimetallic borohydrides synthesized by wet chemistry

We first synthesized bulk quantity of $Mg(BH_4)_2$ to be used as precursor in reactions for bimetallic borohydrides. The hydrogen release temperature of $Mg(BH_4)_2$ is not very high (280–300 °C), amenable to the addition of other metal cations for lower decomposition temperatures. The as-synthesized $Mg(BH_4)_2$ is a complex with ether molecules from the solvent, $Mg(BH_4)_2{\cdot}2Et_2O$ (Fig. 25), readily soluble in dry solvents for further homogeneous reactions toward the targeted multi-cation borohydrides. For the reactions with $LiBH_4$ in solution, the quantitative product analyses by atomic absorption and inductively coupled plasma (ICP) for the metals and boron confirmed the formation of $Li_2Mg(BH_4)_4$ and $Li_{1.3}Mg(BH_4)_{3.3}$ under slightly different experimental conditions (by simply changing the molar ratio of $LiBH_4$ to $Mg(BH_4)_2{\cdot}2Et_2O$). Similarly, the reaction with $Ti(BH_4)_3$ yielded $TiMg_{3.4}(BH_4)_{9.8}$. These wet-chemically synthesized compounds allowed conventional routes to crystallization for unambiguous structural determination. The compounds in powders were characterized by FT-IR and XRD.

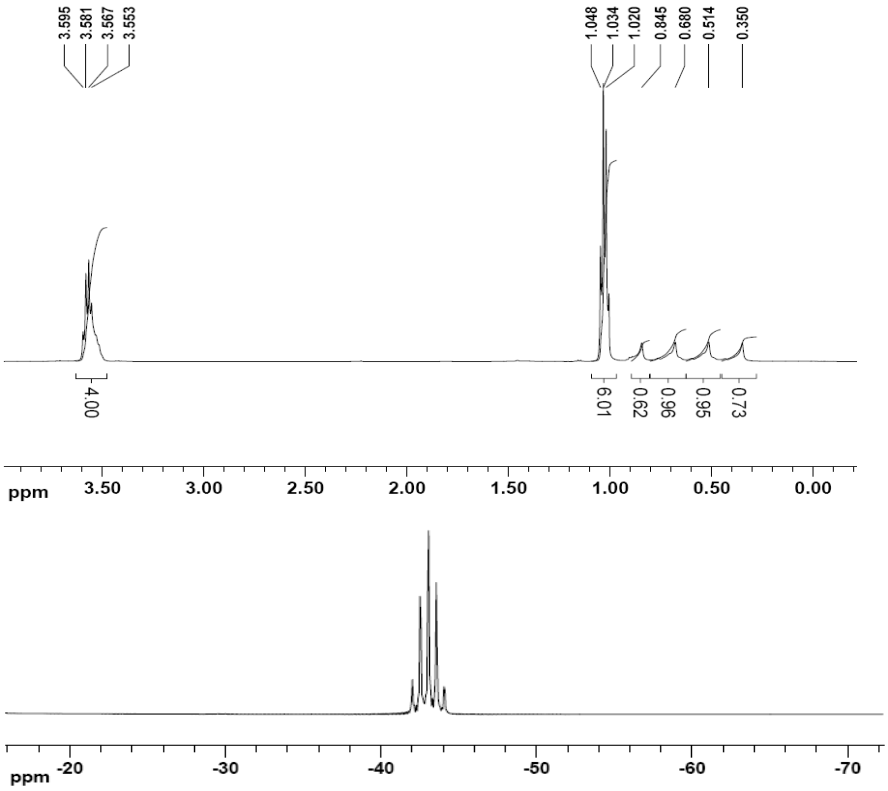

Fig. 25 ^{1}H NMR (top) and ^{11}B NMR (bottom) spectra of $Mg(BH_4)_2.2Et_2O$.

The solid-state infrared spectra of $Mg(BH_4)_2$, $Li_2Mg(BH_4)_4$, $Li_{1.3}Mg(BH_4)_{3.3}$, and $TiMg_{3.4}(BH_4)_{9.8}$ in the 500-3500 cm^{-1} spectral range are presented in Figure 26. Features in the regions of 2200-2400 cm^{-1} and 1110-1310 cm^{-1} are respectively assigned to the stretching and deformation of B-H bonds in the $[BH_4]$ group. The B-H absorption band and bending vibration are both split into three contributions at 2382 cm^{-1}, 2287 cm^{-1}, and 2218 cm^{-1} and two contributions at 1119 cm^{-1} and 1303 cm^{-1}, respectively. The characteristic features of the $[BH_4]$ group were found to be present in both $Li_2Mg(BH_4)_4$ and $Li_{1.3}Mg(BH_4)_{3.3}$, which demonstrated the formation of $[BH_4]$ in both bimetallic boronhydrides. Compared to $Mg(BH_4)_2$, the stretching and bending vibration bands for these bimetallic boronhydrides slightly shifted to higher frequencies (~7 cm^{-1}). For $Li_{1.3}Mg(BH_4)_3$, the B-H absorption band originally at 2382 cm^{-1} for $Mg(BH_4)_2$ was down-shifted and substituted by peaks at 2363 cm^{-1} and 2338 cm^{-1}. These observed shifts might be originated from the loosening of the B-H bond by the electron donation to cation, possibly due to the new coordination of B-H to the lithium cation. In the $TiMg_{3.4}(BH_4)_{9.8}$ spectrum, the stretching of B-H bonds in 2200-2400 cm^{-1} were significantly obscured and attenuated, though the absorption for the deformation of B-H bonds down-shifted to 1024 cm^{-1}. The IR spectral changes are likely due either to changes in the environment surrounding the $[BH_4]^-$ anion or the high reactivity and less stability of $TiMg_{3.4}(BH_4)_{9.8}$.

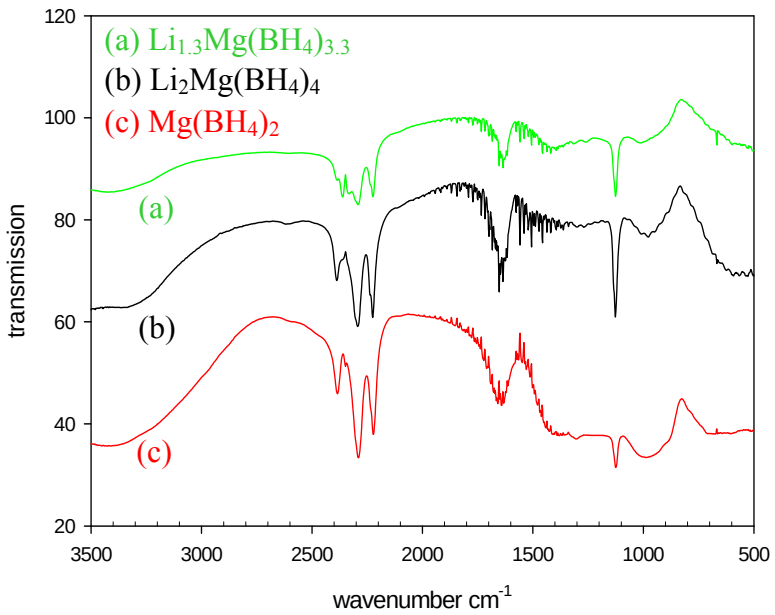

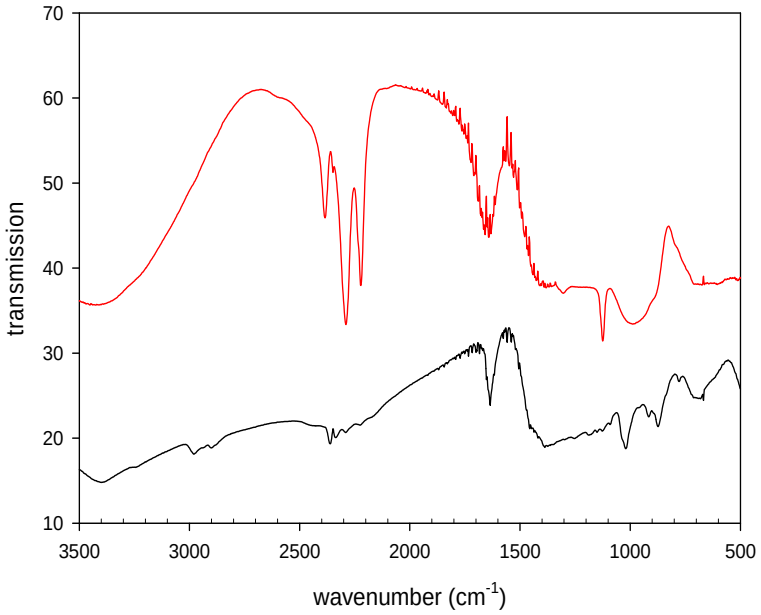

Fig. 26 FTIR spectra of $Li_2Mg(BH_4)_4$, $Li_{1.3}Mg(BH_4)_{3.3}$, and $Mg(BH_4)_2$ (top) and $TiMg_{3.4}(BH_4)_{9.8}$ and $Mg(BH_4)_2$ (bottom).

Powder X-ray diffraction profiles of $Li_2Mg(BH_4)_4$, $Li_{1.3}Mg(BH_4)_{3.3}$ and $TiMg_{3.4}(BH_4)_{9.8}$ products (covered by Kapton film during measurements to protect from oxidation) were compared with those of $Mg(BH_4)_2$ and $LiBH_4$, as shown in Fig. 27. The profile of pure Kapton film was also recorded as background. Except for $TiMg_{3.4}(BH_4)_{9.8}$, all other products showed good crystallinity. The diffraction angles, the *d*-spacing, and the relative peak intensities of $Mg(BH_4)_2$ were similar to those reported in the literature for a pure monophasic α-$Mg(BH_4)_2$ [23,24]. According to the comparison of X-ray results, it seems that the α phase in $Mg(BH_4)_2$ was mostly preserved in $Li_2Mg(BH_4)_4$ and $Li_{1.3}Mg(BH_4)_{3.3}$, though slightly less in the latter. The observed bulge baselines may be attributed to the adducts associated by organic function groups. The absence of strong $LiBH_4$ signals at 18, 24, and 25 degrees in both bimetallic borohydrides and the only minor shifts in some of the signals suggest that the introduction of $LiBH_4$ only slightly changed the crystalline structure of $Mg(BH_4)_2$.

The diffraction peaks of α-$Mg(BH_4)_2$ all disappeared in $TiMg_{3.4}(BH_4)_{9.8}$, suggesting the absence of any long range ordering in the $TiMg_{3.4}(BH_4)_{9.8}$ structure. Similar amorphous structure was also obtained when reacting $TiCl_3$ with $Mg(BH_4)_2$ by ball milling method [25]. The details on the role of $TiCl_4$ and the reaction mechanism have yet to be clarified for further improvement in the properties of Ti-Mg bimetallic boronhydrides.

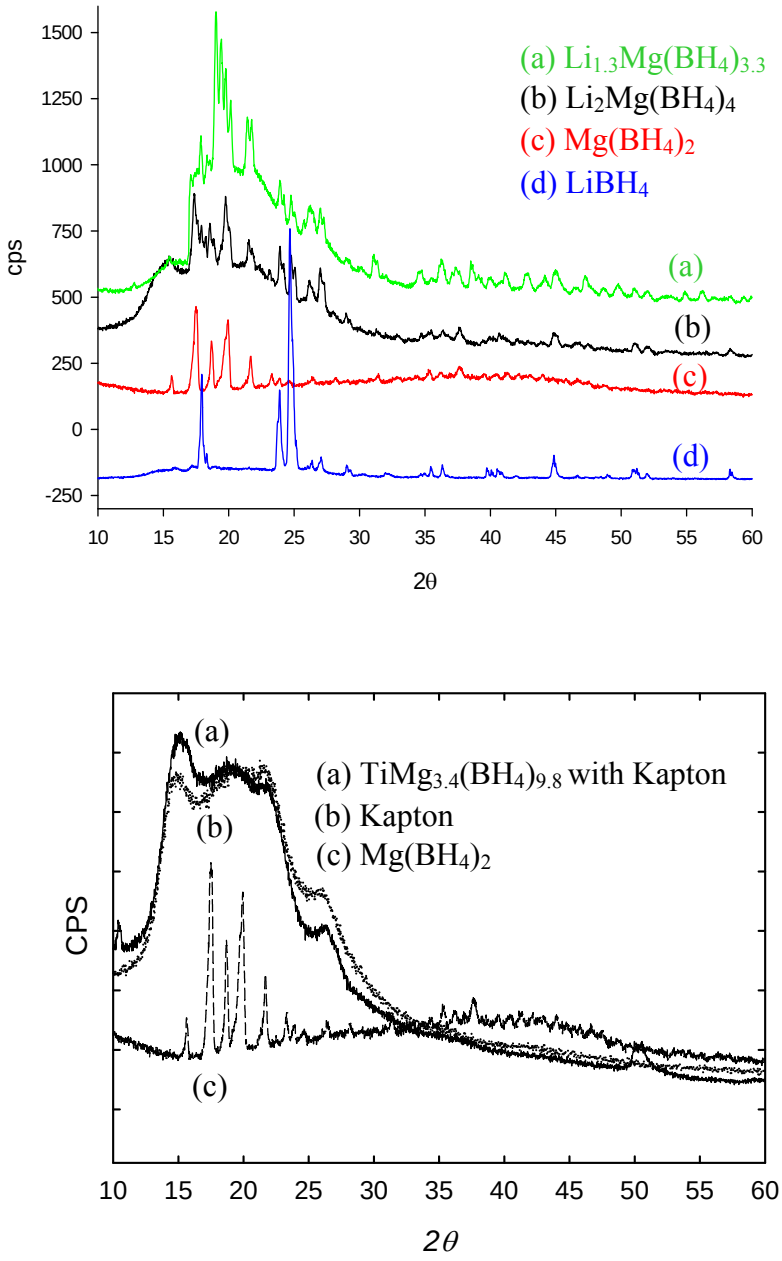

Fig. 27 Powder X-ray profiles of $Li_2Mg(BH_4)_4$ and $Li_{1.3}Mg(BH_4)_{3.3}$ covered by Kapton film (top), and $TiMg_{3.4}(BH_4)_{9.8}$ covered by Kapton film. The profiles of kapton film, and $Mg(BH_4)_2$ and $LiBH_4$ are also shown as references.

3.4 Hydrogen storage behavior of bimetallic borohydrides synthesized by wet chemistry

The TGA-RGA curves for $Mg(BH_4)_2$, $Li_{2.3}Mg(BH_4)_{4.3}$, $Li_{1.3}Mg(BH_4)_{3.3}$, and $TiMg_{3.4}(BH_4)_{9.8}$ are simultaneously compared in Figure 28-30, showing greatly enhanced kinetics for bimetallic borohydrides. The results for all samples indicate a multi-step (more than two steps) dehydriding process, which suggests the presence of several intermediate compounds. For $Mg(BH_4)_2$, the first ~ 4wt% weight loss from 25 to 275 °C is likely due to the evaporation of some residual organic compounds combined with the evolution of very small amounts of H_2, as can be seen from the observed H_2 bulge in RGA curve (Fig.28). The main dehydriding reaction started at approximately 275 °C with a considerable weight loss of approximately 10.73 wt% up to 500 °C, which is consistent with other reports. [15,21,26]. RGA of the gas phase showed that the desorbed gas consisted exclusively of hydrogen, with no trace of B_2H_6 or BH_3. If we assume that all of the desorbed gas from 100 to 500 °C is hydrogen, the total of 14.5 wt% is remarkably similar to the theoretical hydrogen capacity of the material (14.73 wt%). The dehydriding behavior of $Li_{1.3}Mg(BH_4)_{3.3}$ was found to be similar to $Mg(BH_4)_2$, but with an on-set temperature of main dehydrogenation at 50 °C lower, shifting from 300 to 250 °C (Fig.29).

$Li_{1.3}Mg(BH_4)_{3.3}$ and $TiMg_{3.4}(BH_4)_{9.8}$ (Fig. 31) samples exhibited slightly different traces with the corresponding steps significantly shifted toward the lower temperatures. At a given temperature, the amount of hydrogen evolved from these samples was generally higher than that from the pristine $Mg(BH_4)_2$ respectively. $Li_2Mg(BH_4)_4$ (Fig.30) and $TiMg_{3.4}(BH_4)_{9.8}$ begun evolving hydrogen from 80 and 100 °C and the total weight losses upon 500 °C were determined to be about 19 wt% and 24 wt% respectively. These samples also showed series of bumps at 250 °C-350 °C due to melting and foaming. Similar to $Mg(BH_4)_2$, only hydrogen was detected from the evaluation of gas phase and no trace of B_2H_6 or BH_3 were found. It should also be noted that no sharp H_2 peaks were observed in RGA as typical dehydriding does. The H_2 dull peak may represent different dehydriding process, in which hydrogen was gradually released from whole range of temperatures rather than at certain defined temperatures. The large weight losses can not be solely attributed to hydrogen evolution. This may also be attributed to the evolution of other gases undetected by our RGA and/or the escape of a part of the sample during foaming.

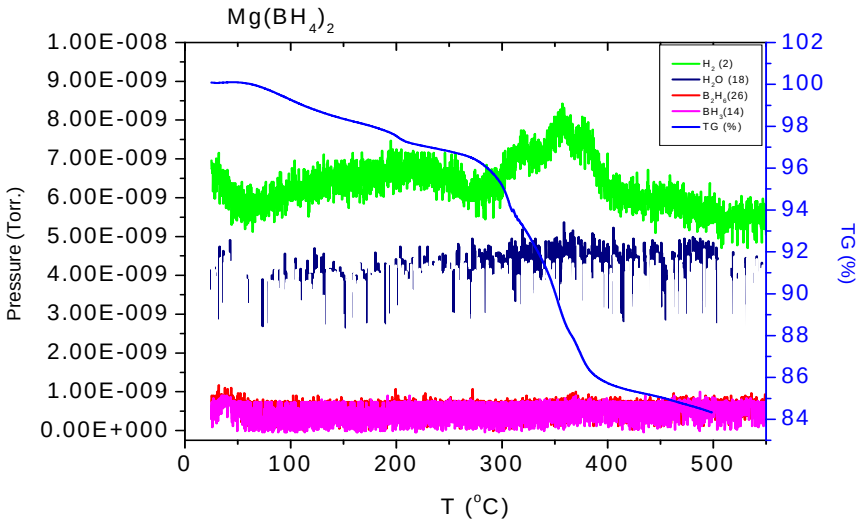

Fig.28 TGA-RGA spectra of $Mg(BH_4)_2$

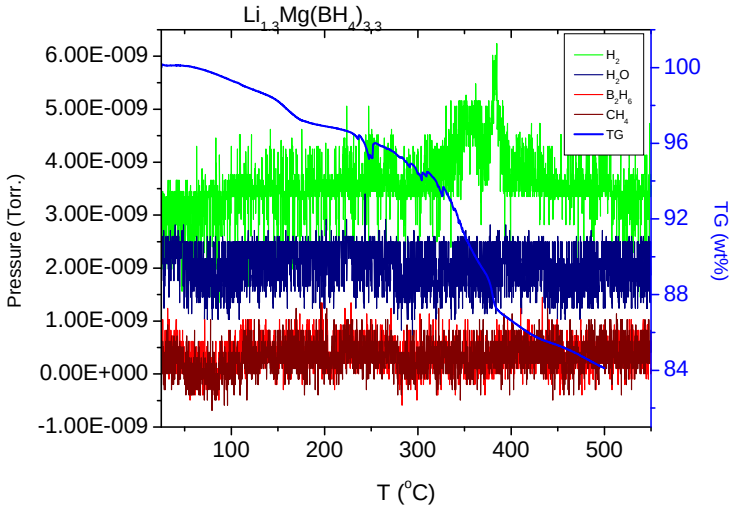

Fig.29 TGA-RGA spectra of $Li_{1.3}Mg(BH_4)_{3.3}$

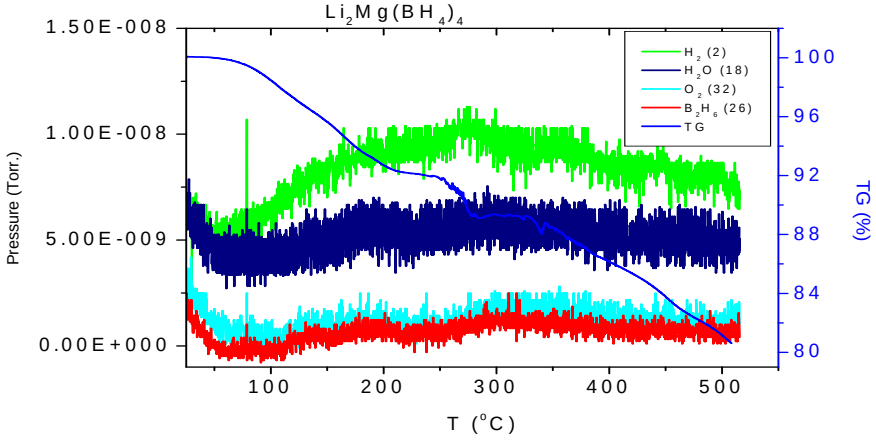

Fig.30 TGA-RGA spectra of $Li_{2.3}Mg(BH_4)_{4.3}$

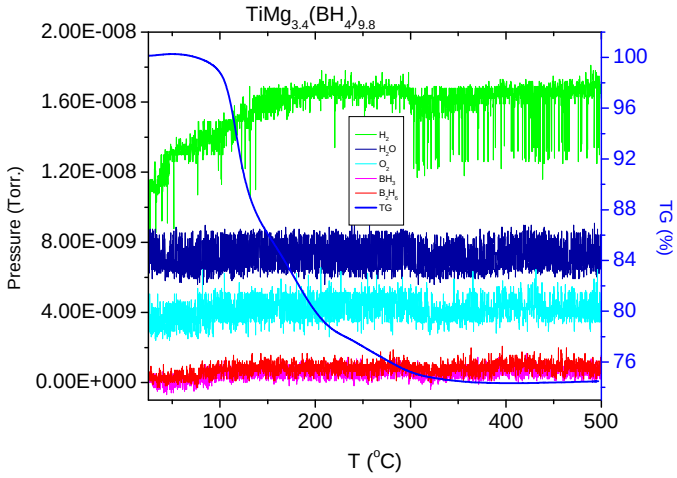

Fig.31 Hydrogen absorption of $TiMg_{3.4}(BH_4)_{9.8}$

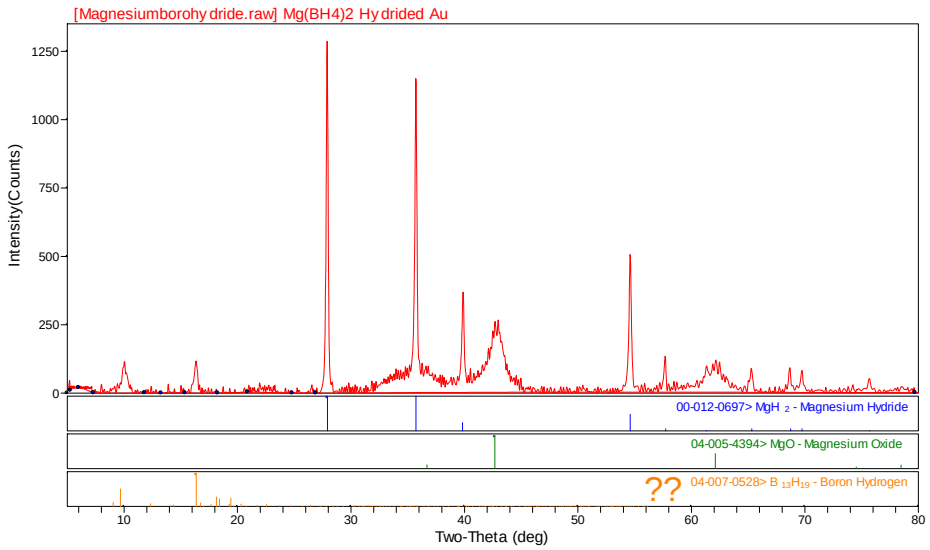

Fig.32 XRD of the rehydrided $Mg(BH_4)_2$

5. CONCLUSION

The bimetallic borohydrides synthesized by wet chemistry demonstrated lower dehydrogenation temperature (100-300^{o}C) and adequate storage capacity (8-12 wt%) as predicted. By dissolving precursors in the organic solvent, the [BH_3] tetrahedrons and the cations, such as Li, Mg and Ti, can apparently rearrange their coordination to form new complexes of bimetallic borohydrides. It is demonstrated that the wet chemistry is a viable process for synthesis of bimetallic borohydrides. Their stability varies largely and mainly depends on the selection of the second metal. $Mg(BH_4)_2$ doped by Ti tends to be more instable and less reversible than one doped by Li. The new bimetallic borohydrides were capable of reabsorbing hydrogen at 300^{o}C and 100 bar. There is a room to tune the stability and reversibility of $Mg(BH_4)_2$ by carefully selecting appropriate second metal elements. The ball milling sintering and high pressure milling processes were not able to synthesize bimetallic borohydrides due to insufficient chemical reaction to incorporate the second metal in M-(BH4)x complex.

Acknowledgement

This project is financially supported by NNSA PDRD program and General Motors Corporation. Savannah River National Laboratory is operated by Savannah River Nuclear Solution for US Department of Energy under contract DE-AC09-08SR22470.

References:

[1] A.Muller, L. Havre et al, US Patent 4193978, (1980)
[2] A. Zuttel, S.Rentsch et al, J.Alloy.Compd. 356-357(2003)515-520
[3] M. Au, A.Jurgensen et al, J.Phys.Chem.B 110(2006)7062-7067
[4] M.Au, A. Jurgensen et al. J.Phys.Chem.B 110(2006)26482-26487
[5] J.Vajo and S.Skeith, J.Phys.Chem.B. 109 (2005) 3719-3722
[6] F.Pinkerton, G. Meisner et al, J.Phys.Chem.B 110(2005)6-8
[7] S-A Jin et al, Scirpta Materialia, 58(2008)963-965
[8] Y. Zhang, W.-S. Zhang, A.-Q.Wang, L.-X. Sun, M.-Q. Fana, H.-L. Chu, J.-C. Sun, T. Zhang, Int. J. Hydrogen Energy **32** (2007) 3976 – 3980.
[9] S.Orimo,Y. Nakamori, et al, "Dehydriding and rehydriding reactions of $LiBH_4$", J.Alloy.Comp. 404-406 (2005)427
[10] X-D Kang et al, Appl.Phys.A 89(2007) 963-966
[11] S.G.Shore and R.W.Parry, J.Am.Chem.Soc. 80(1958)8-12
[12] H.I.Schlesinger et al, J.Am.Chem.Soc.75(1953)199-204
[13] H.Hoekstra and J.J.Katz, J.Am.Chem.Soc. 71(1949)2488-2492
[14] H.I.Schlesinger et al, J.Am.Chem.Soc.75(1953)209-213
[15] E. Wiberg, R Bauuer et al, Z. Naturforsch. 1950,5b, 397
[16] J.Jensen e tal, J. Am.Chem.Soc. (1988) 110, 1643-1644
[17] V.V.Volkov et al, Proceeding of the 2 Japan-Soviet Symposium on Mechanochemistry,1988.231
[18] H.R.Hoekstra et al, J.Am.Chem.Soc. 1949. 71. 2488
[19] J.Jensen et al, J.Am.Chem. 1988. 110. 1643
[20] C.Jensen, "Fundamental study of high capacity reversible metal hydrides", DOE Hydrogen program annual review meeting, 5/16/2007
[21] J-C.Zhao, M.Andrus et al, "Light weight intermetallics for hydrogen storage", DOE Hydrogen program annual review meeting, 5/16/2007
[22] Y.Nakamori, H.Li, K. Miwa, S-I. Towata and S-I.Orimo, Materials Transactions, V47, N8(2006)1898-1901
[23] P. Zanella, L. Crociani, N. Masciocchi, G. Giunchi, *Inorg. Chem.* 46, (2007**),** 9039-9041.
[24] K. Chlopek, C. Frommen, M. Fichtner, *J. Mater. Chem*., 17, (2007), 3496-3503.
[25] H.-W. Li, K. Kikuchi, K. Miwa, S. Orimo. *Scripta Materi.* 57, (2007), 679-682.
[26] W. Heisenberg, W. Bothe et al, Z.Naturforsch. 7b, (1952), 58
[27] M.Au et al, J.Phys.Chem.C 112, 2008, 18661-18671
[28] S-J. Huwang et al, J.Phys.Chem.C 112, 2008, 3164-3169

Supporting materials

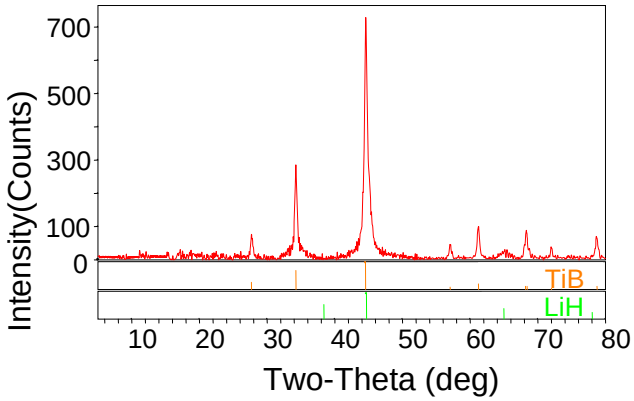

Fig.1 XRD of ball milled $1.5LiH+0.5TiB_2+0.2B_{10}H_{14}$

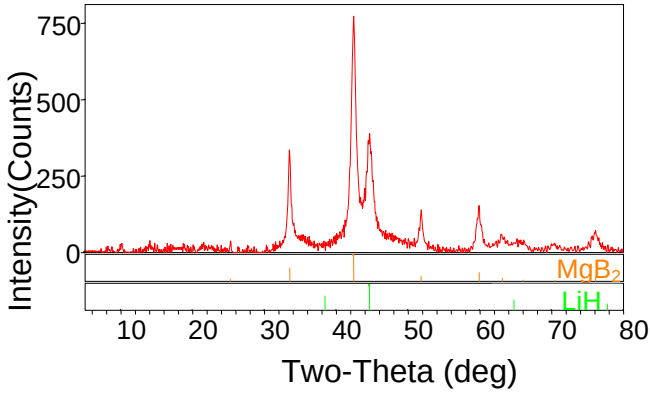

Fig.2 XRD of ball milled $LiH+0.5MgB_2+0.3B_{10}H_{14}$

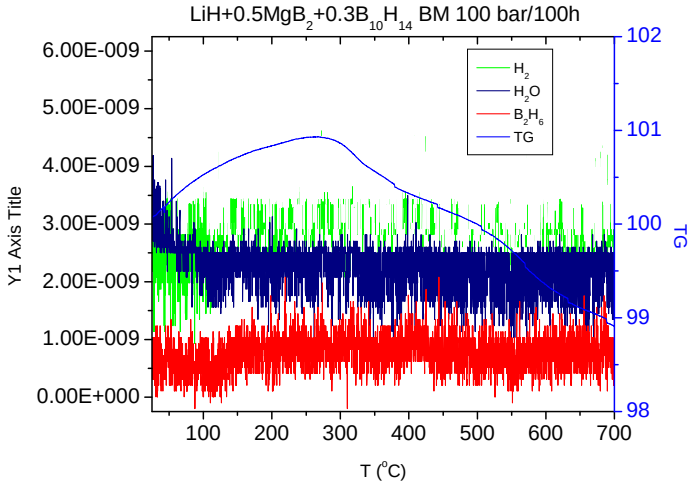

Fig.3 TGA-RGA spectra of sample $LiH+0.5MgB_2+0.3B_{10}H_{14}$

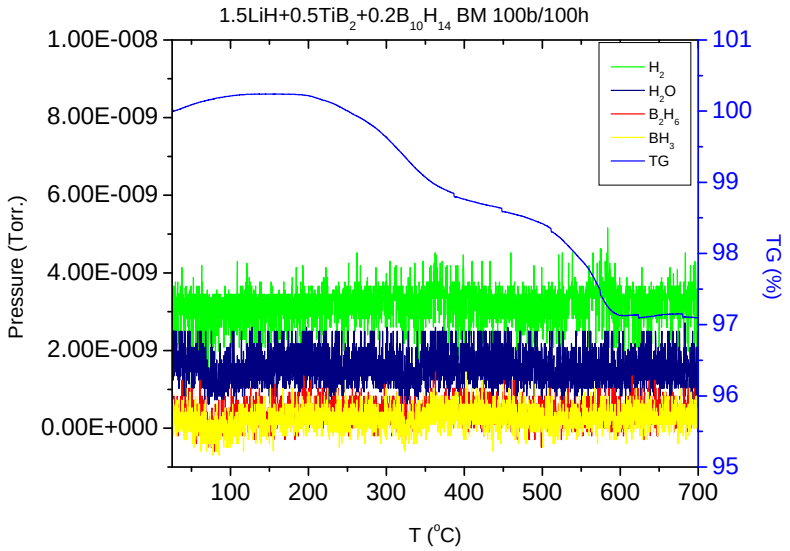

Fig.4 TGA-RGA spectra of sample LiH+0.5TiB_2+0.2$B_{10}H_{14}$